ICANS-XI International Collaboration on Advanced Neutron Sources
KEK, Tsukuba, October 22-26, 1990

INVESTIGATION AND GROWTH OF MULTILAYERS

P. Böni and I. S. Anderson
Paul Scherrer Institut
CH-5232 Villigen PSI, Switzerland

R. Hauert
EMPA
CH-8600 Dübendorf, Switzerland

P. Ruterana
EPFL
CH-1015 Lausanne, Switzerland

K. Solt
Landys & Gyr
CH-6301 Zug, Switzerland

B. Farnoux
Laboratoire Léon Brillouin
CEN-Saclay
F-91191 Gif-sur-Yvette Cédex, France

G. J. Herdman and J. Penfold
Rutherford Appleton Laboratory
Chilton, Didcot, Oxon OX11 0QX, United Kingdom

O. Schärpf
Institut Laue Langevin
F-38042 Grenoble, Cedex, France

ABSTRACT

Following the pioneering work on multilayers for neutron mirrors and polarisers performed at ILL, there has been a recent upsurge in the efforts to produce high quality mirrors on a large scale. Modern analytical techniques allow the detailed structure of thin metallic films and their interfaces to be investigated and related to the deposition parameters. By combining such studies with neutron reflection measurements, it is possible to determine the effect of structural properties and defects on the neutron reflectivity and thus eventually refine the deposition technique and parameters. Results will be presented on multilayers

produced by various methods and studied by neutron spectroscopy, Auger depth profiling, and transmission electron microscopy.

I. INTRODUCTION

Neutron guide tubes provide an efficient transport of neutrons to a wide variety of instruments in areas with low backgrounds.[1] Up to now most of the guides have been coated with natural Ni (Ref. 2) having a critical angle of reflection $\theta_c/\lambda = 1.7$ mrad/Å (6 min/Å). Recently ^{58}Ni has replaced natural Ni as a guide coating [3] with the advantage that the critical angle is increased by a factor $m = 1.2$ resulting in flux gains up to m^2 (Ref. 4). More recent progress in this area suggests that it may become possible to produce supermirrors with an excellent reflectivity ($R > 0.98$) and with even larger θ_c, namely $m \geq 1.5$. Guides coated with such supermirrors, in addition to the overall flux gains that may be achieved, allow increased transmission at short wavelengths, suggesting the feasibility of their use in normal beam tubes.

These properties are particularly important at a continuous spallation source like SINQ at PSI, where the production of high energy neutrons necessitates rather bulky target shielding. Supermirror coated guides and beam tubes may efficiently transmit even short wavelength neutrons over the large distances required. More effective use of the available neutrons at the instruments may be achieved by the use of additional optical elements such as polarizers, focussing devices, monochromators, band pass filters etc., which also depend on the development of artificial multilayers. For this reason we have an ongoing project to study the production and the properties of thin films for neutron optics.

The results we present here review some aspects of our work on Ni/Ti multilayers produced by various deposition techniques and characterised using a number of analytical techniques such as neutron reflection, transmission electron microscopy (TEM), and Auger depth profiling.

II. EXPERIMENTAL

Our investigations have been based on the study of Ni/Ti multilayers of constant bilayer spacing (usually between 100 and 140 Å) deposited onto polished silicon wafers with the aim of determining the effect of the deposition parameters on the structure and reflectivity of the multilayer stack. Some characteristics of the deposition techniques that we have used may be summarised as follows:

Evaporation: The target is heated in a high vacuum chamber ($10^{-5} < p_i < 10^{-6}$ mbar) to produce a vapour pressure of the order of 10^{-2} mbar. The evaporated particles have thermal energies (0.05 to 0.5 eV) and follow an almost collisionless path to the substrate. Due to the very non linear dependence between vapour pressure (hence deposition rate), and temperature the process is difficult to control and thickness monitors must be used. Moreover the rather low energies of the incident particles at the growing film leads to underdense structures usually under tensile stress.

Magnetron sputtering: In this case the atoms are sputtered from the surface of a target due to bombardment by energetic inert gas ions produced in a glow discharge plasma which is confined to the target surface by a magnetic field. The sputtered atoms are ejected with considerable kinetic energy, 50 - 100 times higher than in vacuum evaporation, with an average energy of the order of 10 - 40 eV. Additionally, reflected working gas atoms, which have been neutralised at the target by emitted electrons, may reach the substrate with a considerable fraction of their initial energy so that the growing film may be significantly modified by the bombardment by energetic particles. The final energies of both the sputtered species and the

reflected working gas atoms at the substrate will depend on the product of the working gas pressure (usually in the range 1 - 5 mbars) and the distance from target to substrate so that these parameters may be used to control film growth properties.

Ion Beam Sputtering: The glow discharge sputtering described above is limited in the sense that target current density and the particle energy cannot be independently controlled except by varying the working gas pressure. Ion beam sputtering permits independent control over the energy and current density of the bombarding ions. The sputtering target is arranged to obliquely intercept an ion beam of given energy and flux density that is created by an independent ion source. Ion beam sources permit sputtered coatings to be deposited at very low working gas pressures ($\simeq 0.1$ mbar) onto substrates which are not in contact with the plasma so that uncontrolled particle bombardment and therfore heating rates may be minimised. In addition secondary ion sources may be used (Ion beam assist) to provide direct, controlled bombardment of the growing film during deposition in order to modify its properties.

The reflection profiles of the samples were measured on neutron reflectometers installed at the pulsed spallation source ISIS and at the Orphée reactor in Saclay. Such instruments have the particular advantage of using fixed sample geometry and therefore constant illumination, the profile being determined by a wavelength scan. Additional measurements of the reflectivity of the Bragg peak have been performed on the S3 double axis spectrometer at the Institut Laue Langevin[2] using a fixed wavelength $\lambda = 7.2$ Å. In this case special precautions were taken to confirm that the illumination remained constant by using extra large samples.

In the present work we have characterized the samples using TEM results obtained on a Philips EM430ST microscope which provides a point resolution better than 0.2 nm. The cross-section sample preparation was carried out by ion-milling at liquid-nitrogen temperature ensuring minimal damage to the layer structure.[5] Both dark field and bright field images were obtained in addition to electron diffraction patterns, yielding detailed information on the crystalline structure and morphology of the layers.

The Auger depth profile was performed at EMPA. A Perkin Elmer PHI-4300 high resolution scanning Auger system was used. The analysis was performed on a $5 \times 15\ \mu m^2$ area, at a primary electron beam voltage of 5.0 kV and at a beam current of 500 nA. The CMA (Cylinder Mirror Analyzser) was operated at 0.6% resolution. Profiling was done by sputtering for 15 s inbetween Auger spectra by Ar-sputtering at 4.5 kV over a 5×5 mm^2 rectangular area. The sputter rate was calibrated to 8 nm/min on a SiO_2 standard reference. The base pressure in the analysis chamber was $5 \cdot 10^{-10}$ mbar. The depth resolution of 20 Å could not be reached due to ion-mixing caused by the Ar-sputtering while depth profiling. By the same reason some of the Ti and Ni was driven into the Si substrate during Auger depth profiling (Knock-on effect). For details see Ref. 6.

III. RESULTS

We have made Ni/Ti multilayers using all the deposition methods mentioned in the previous paragraph and have analyzed their structure and reflectivity. As a first comparative step the Bragg peak reflectivities of various specimens were measured using the S3 spectrometer at the ILL. We show the results of these measurements in Table 1. and compare them with theoretical estimates based on the measured bilayer thickness. Also listed in the tables are the main deposition parameters used for each sample.

The comparison between the experimental and theoretical reflectivities clearly shows that the evaporated samples were inferior to the sputtered ones. The Bragg peak of sample

E1 has large wings, indicating that the layer thicknesses d_i (i = Ni, Ti) are not uniform a result confirmed by TEM (see later). Moreover, d_i depends even on the position of the samples inside the apparatus therefore the evaporation process is not homogenous.

The high rate sputtered samples have generally a significantly better reflectivity than the low rate sputtered samples. Decreasing the pressure during sputtering at high rate increases the reflectivity of the multilayers, whereas etching turns out to be a less important parameter. The reflectivity of the ion beam sputtered samples is rather low. Neutron reflectometer and TEM results show that this is primarily due to poor thickness control during deposition.

Table 1: Characteristic properties of the evaporated and sputtered samples. p_i is the pressure, v the deposition rate, R is the measured reflectivity, and R_{th} is the calculated reflectivity, based on the measured bilayer thickness $2D$.

Evaporation (20 bilayers Ni/Ti 50 Å)

sample	etch	p_i (mbar)	v (Å/s)	D (Å)	R (%)	R_{th} (%)
E1	no	$\simeq 10^{-5}$	10	51.2	40	82

Low rate sputtering (20 bilayers Ni/Ti 50 Å)

sample	etch	p_i (mbar)	v (Å/s)	D (Å)	R (%)	R_{th} (%)
ML1	no	$4 \cdot 10^{-3}$	Ni 1.42, Ti 3.3	51.1	67	82
ML2	no	$4 \cdot 10^{-3}$	Ni 1.42, Ti 3.3	52.5	63	85

High rate sputtering (15 bilayers Ni/Ti 50 Å)

sample	etch	p_i (mbar)	v (Å/s)	D (Å)	R (%)	R_{th} (%)
MH1	yes	$6 \cdot 10^{-3}$	17.5	46	46	53
MH2	yes	$6 \cdot 10^{-3}$	17.5	46	41	53
MH3	yes	$3 \cdot 10^{-3}$	18.7	48.5	60	60
MH4	yes	$3 \cdot 10^{-3}$	18.7	48	57	59
MH5	no	$3 \cdot 10^{-3}$	18.7	49	57	61.5
MH6	no	$3 \cdot 10^{-3}$	18.7	48	56	59

Ion beam sputtering (15 bilayers Ni/Ti 50 Å)

sample	ion ass.	p_i (mbar)	v(Å/s)	D (Å)	R (%)	R_{th} (%)
I1	no	$1.5 \cdot 10^{-4}$	Ni 1.8, Ti 1.4	53	44	71
I2	no	$1.5 \cdot 10^{-4}$	Ni 1.8, Ti 1.4	51	43	67
I3	yes	$1.5 \cdot 10^{-4}$	Ni 0.95, Ti 0.72	56	49	77
I4	yes	$1.5 \cdot 10^{-4}$	Ni 0.95, Ti 0.72	55	51	75

Ion beam parameters:			
	sputtering	150 mA	1000 eV
	assist	75 mA	250 eV

In order to understand the origin of the widely differing reflectivities of our samples we have studied the structure of the layers by means of high resolution TEM. The results for

the evaporated samples show that only the first few layers are of good quality. The following layers become increasingly wavy due to the growth of large crystal grains within the layers, and even island formation starts. This explains the low reflectivity of the evaporated samples. Similar TEM observations have been made on the low rate sputtered samples: The Ni and Ti layers are crystalline with a preferred orientation in the [111] direction and the [002] direction, respectively. The build up of roughness caused by large crystallites eventually leads to the breakdown of the regular layer structure.

The TEM results on the high rate magnetron sputtered samples are particularly interesting. Fig. 1a shows as an example the excellent morphology of the layers of a sample that was made under low pressure conditions. A close inspection of the TEM-pictures shows that the Ni layers are crystalline with a preferred orientation [111] as before. The Ti layers, however are crystalline for high pressure conditions and amorphous for low pressure conditions. This observation correlates with the neutron reflectivities, namely the amorphous Ti layers seem to smooth out irregularities in the layer stack and yield samples with a higher reflectivity.

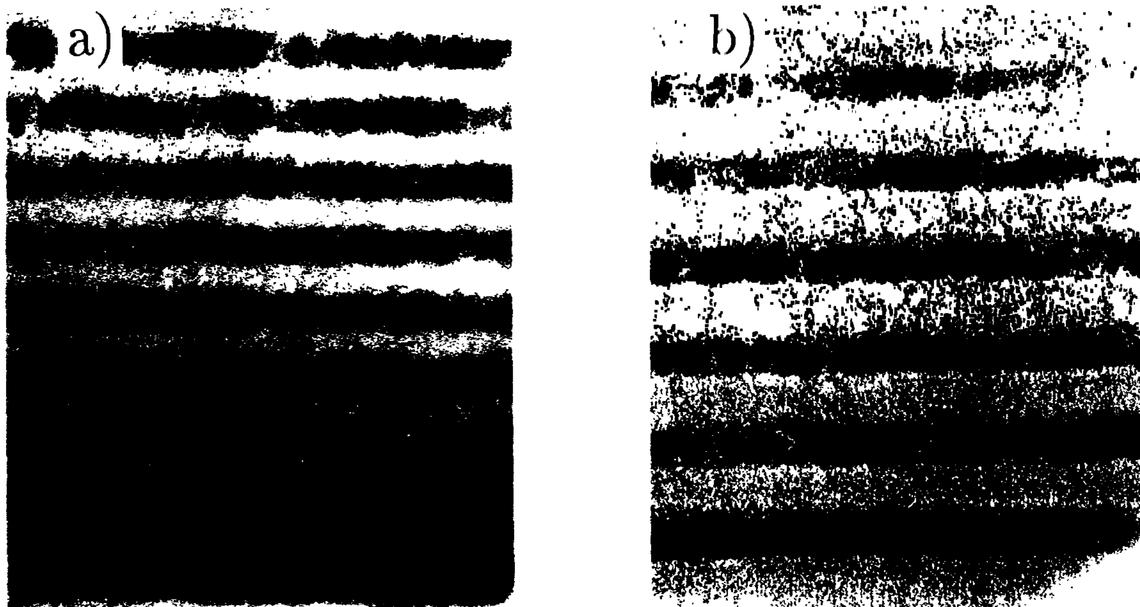

Fig. 1. *a) TEM photograph of the high rate sputtered multilayer MF5. The bright layers are composed of amorphous Ti ($\simeq$ 55 Å), the dark layers ($\simeq$ 44 Å) are composed of small grained Ni crystals. b) TEM photograph of an ion beam sputtered sample (15 bilayers Ni/Ti, $d_i \simeq 50$ Å) which was concurrently bombarded by a second ion beam. Note the well defined interfaces.*

In Fig. 1b we show a TEM for an ion beam sputtered sample. The appearance of the layers is impressive. Again the Ni layers are crystalline ([111] in the layer) and the Ti layers are mostly amorphous with some evidence of crystallinity in the center. The samples deposited with ion beam assist seem to have Ti layers that are completely amorphous and the Ni layers have a reduced grain size. However, because of the poor thickness control it is not possible to judge unambiguously the effects on the reflectivity.

In addition we also studied the atomic composition of the high rate sputtered multilayers by means of Auger depth profiling. In Fig. 2 we show a typical scan. The resolution of the instrument is only approximately 50 Å due to ion mixing during Ar sputtering. The dominant substances are clearly Ni and Ti, namely $c_{Ni} \simeq 54$ at.% and $c_{Ti} \simeq 42$ at.%. These numbers

correlate nicely with the fitted thicknesses from the reflectivity measurements to be discussed below, namely $d_{Ni} = 54.8 \pm 0.2$ Å and $d_{Ti} = 44.2 \pm 0.1$ Å. Since Argon gas was used for sputter etching, its concentration could not be directly determined, however an upper limit of the analysis yields $c_{Ar} < 2.2$ at.%. Furthermore, concentration limits for carbon and nitrogen impurities can be given from ESCA spectra: $c_C < 1.3$ at.%, and $c_N < 0.4$ at.%.

An interesting behaviour is observed for the concentration of oxygen. The mean concentration is $c_O \simeq 2.4$ at.%. It shows a periodic oscillation in time (depth), similar as Ni and Ti. A closer inspection of Fig. 2 shows that the oxygen content rises at the beginning of the Ti layers. Obviously, Ti acts as a getter material and absorbes O_2 from the environment, in contrast to Ni. This observation is particularly interesting because this effect offers the possibility to create a diffusion barrier TiO_2 between the Ni and Ti layers by controlled implementation of O_2.[7] Indeed, reflectivity and TEM measurements indicate that the interface of Ti on Ni (10 Å) is sharper than the interface of Ni on Ti (14 Å).

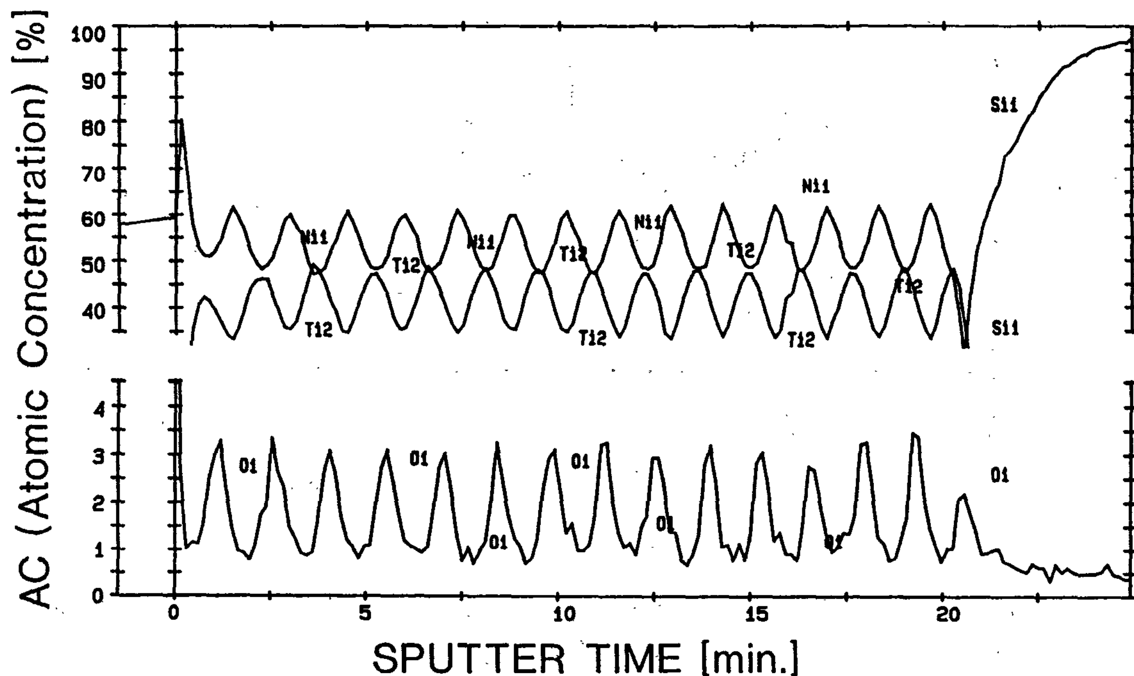

Fig. 2. *Auger depth profile of a high rate sputtered sample containing 15 bilayers Ni/Ti. The signals for Ni and Ti are exactly out of phase, whereas the O_2 signal appears only at the beginning of each Ti layer.*

Finally we investigated in a preliminary study the temperature dependence of some high rate sputtered samples. In Fig. 3 we show typical reflection profiles measured at temperatures of 30° and 149°C and an angle of incidence $\theta = 1.05°$. The peak at 3.57 Å is the principal Bragg peak corresponding to a d-spacing of 99.0 Å of the multilayer. The solid line is a fit to the data taking into account only the data points between 3 Å and 11 Å. The data at longer wavelength is possibly strongly influenced by the detailed structure of the substrate interface what we have so far been unable to model satisfactorily. The fitting function is based on conventional optics[8], including refraction and diffraction. The fitted parameters are a normalisation constant for the neutron intensity, the angular resolution of the instrument $\delta\theta$ and the thicknesses d_i, i = Ni, Ti (4 parameters). For the scattering densities g_i we used the bulk values of Ni ($9.4 \cdot 10^{-6}$ Å^{-2}) and Ti ($-1.95 \cdot 10^{-6}$ Å^{-2}). Fitting g_i did not significantly

improve the fits because g_i and d_i are strongly correlated. The fits yielded $d_{Ni} = 54.8 \pm 0.2$ Å and $d_{Ti} = 44.2 \pm 0.1$ Å. The agreement between the fits and the data is excellent within the restricted range of λ. An increased angular resolution $\delta\theta$ which varies between 0.045^0 and 0.072^0 for various high rate sputtered samples may be attributed to bending of the samples.

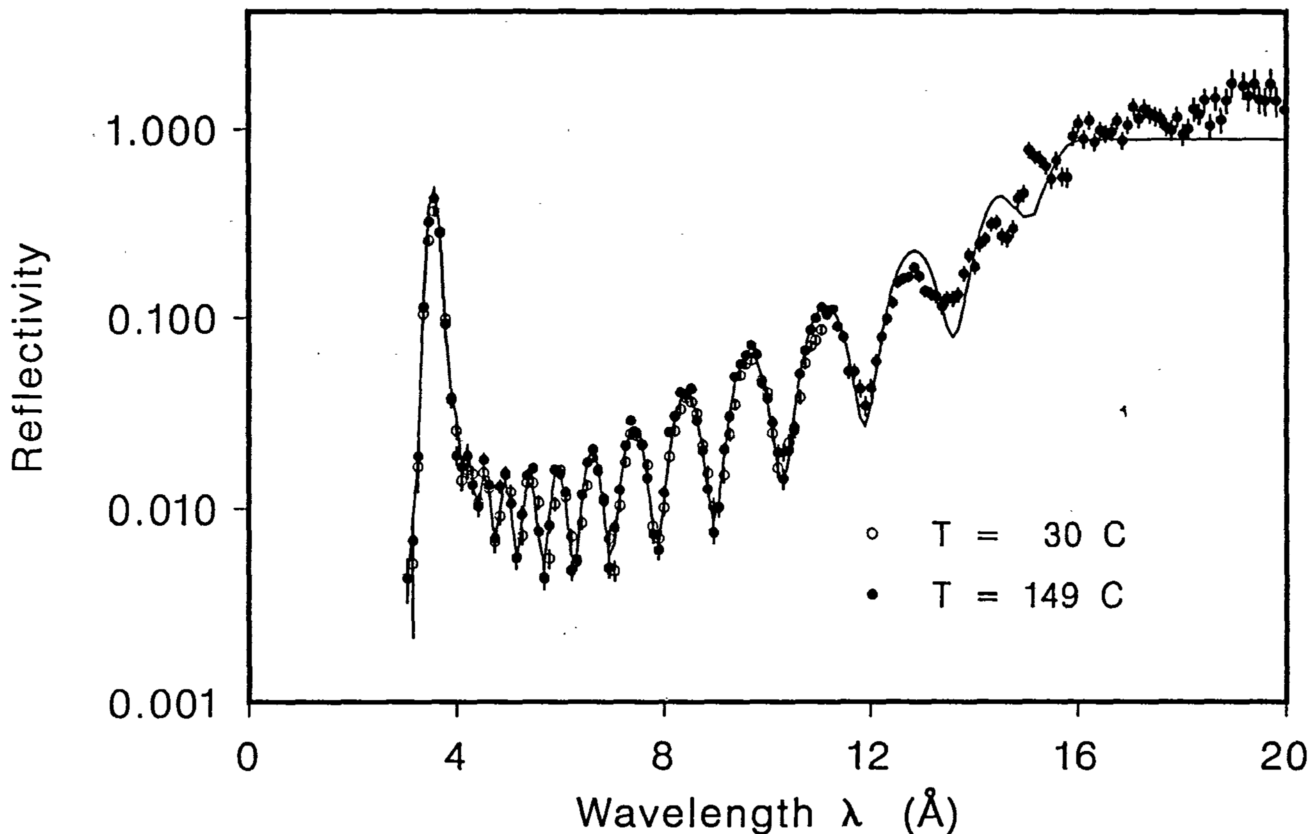

Fig. 3. *Measured reflectivities of the high rate sputtered multilayer MF5, containing 15 bilayers of Ni/Ti (50 Å), versus wavelength. The angle of incidence is* $\theta = 1.02°$. *The solid line is a fit to the 149° C data, using data within the range* $3 < \lambda < 11$ *Å.*

The reflectivity increases slightly when the samples were heated from room temperature to 149 C. The fits indicate that the *d*-spacings decreased by roughly 0.5 % and $\delta\theta$ decreased. The former effect is equivalent to an increase of the density of the multilayer stack whereas the latter effect may be related to a reduced bending of the Si wavers. We have initiated further measurements to address the dependence of a heat treatment on the layer properties in more detail by means of both neutron reflection and TEM with micro-analysis.

IV. DISCUSSION

In the previous sections we have demonstrated that the morphology and the reflectivity of the artificial multilayers depend strongly on the physical conditions near the substrate during the deposition process. Let us summarize the previous results as follows. All samples with amorphous Ti layers and small Ni grain sizes show a nominally better reflectivity. Large grains favour buckling of the layers and island formation. We speculate that the ideal multilayer would consist of amorphous layers only. The amorphicity of Ti is linked to the energy of the

incident sputtered atoms, the energy of the reflected neutral working gas atoms, and the rate at which the sputtered species arrive at the growing film.

High rate sputtering favours small grain sizes possibly because the crystallites do not find time to grow under the intense bombardment of the energetic sputtered particles. Ion beam sputtering, on the other hand, yields well defined layers, although the growth process is slow. However, because the pressure is very low, $p_i = 1.5 \cdot 10^{-4}$ mbar, the sputtered particles have a higher energy (although a lower flux) and reduce the grain size. This effect can be independently enhanced by means of ion assisted sputtering. We conclude that high rate, low pressure, and high energy of the sputtered particles favour the growth of high quality Ni/Ti multilayers.

Presumably the ion beam technique is the most promising for future multilayer production due to its flexibility in optimizing independently the various deposition conditions. However, systems which are capable of coating the large surface areas necessary for a neutron guide system, exist only as prototypes and may require some years of development before full optimization is achieved.

Rather, based on the surface area required for the SINQ quide system, taking into account the planned commissioning schedule and following the philosophy of acquiring only fully tested equipment we have opted to buy a commercially available magnetron sputtering system, which is due for delivery in Spring 1991. The machine comprises a load lock module and a deposition chamber in which the substrates are translated below three high power DC magnetron targets to produce coatings with a design uniformity of 3% over an area of 500×360 mm^2.

On our present schedule we will benefit from approximately 15 months of time to optimize the deposition characteristics before guide production must begin. Besides we will proceed with various other lines of investigations such as smoothing layers, alternative high contrast materials, substrate effects and of course long term stability with respect to thermal and radiation cycling.

OBITUARY

During the preparation of this manuscript we (ISA and PB) were deeply saddened to hear of the untimely decease of our colleague John Herdman, following an intermittent period of illness. We are greatly indebted to him for his very thorough work on describing the neutron reflection profiles from which we learned a great deal. We wish to express our sincere respect for him as a scientist and colleague.

REFERENCES

1. H. Maier-Leibnitz and T. Springer, Reactor Sci. & Techn. **17**, 217 (1963).
2. Guide to Neutron Research Facilities at the ILL, ed. by H. Blank and B. Maier, December 1988.
3. K. Werner, T. Springer, and J. Duppich, IAEA-CN-46/54P, 393 (1985).
4. I. S. Anderson, SPIE Vol. **983**, 84 (1989).
5. P. Ruterana, J.-P. Chevalier, and P. Houdy, J. Appl. Phys. **65**,3907 (1989).
6. Practical Surface Analysis, Eds. D. Briggs, M. P. Seah, John Wiley & Sons (1983).
7. O. Schärpf, Physica B **156 & 157**, 631 (1989).
8. S. Yamada, T. Ebisawa, N. Achiwa, T. Akiyoshi, and S. Okamoto, Annu. Rep. Res. Reactor Inst. Kyoto Univ. Vol. **11**, 8 (1978).

Q(T.Ebisawa): In the case of evaporation technique, vacuum pressure control is important. How many pressure do you have. The pressure used is the optimum condition?

A(P.Boni): The pressure p_i in the deposition chamber was chosen in between $10^{-5} \sim 10^{-6}$mbar. p_i may not have been at the optimum value.